



ELSEVIER

Nuclear Instruments and Methods in Physics Research B 135 (1998) 430–435

NIM B
Beam Interactions
with Materials & Atoms

Influence of chemical structure and beam degradation on the kinetic energy of molecular secondary ions in keV ion sputtering of polymers

A. Delcorte^{*}, P. Bertrand

Unité de Physico-Chimie et de Physique des Matériaux, Université Catholique de Louvain, PCPM, 1 pl. Croix du Sud, B-1348 Louvain-la-Neuve, Belgium

Abstract

The secondary ions sputtered from thin polymer films under 15 keV, Ga⁺ bombardment were mass- and energy-analysed by means of a Time-of-Flight Secondary Ion Mass Spectrometer. The comparison between aliphatic (polyisobutylene) and aromatic polyolefins (polystyrene) allows to propose a process of ion emission in which the mean kinetic energy of the secondary ions is related the degree of fragmentation with respect to the polymer target structure. The important yield decrease and the broadening of the kinetic energy distributions (KEDs) observed for the C_xH_{2x} ions sputtered from pre-bombarded polyisobutylene (10¹²–10¹⁵ ions/cm²) are explained in terms of physico-chemical modification of the surface. The fast metastable decay of molecular ions in the acceleration section of the spectrometer is also investigated. © 1998 Elsevier Science B.V.

Keywords: Secondary ion mass spectrometry; Ion emission; Metastable ions; Kinetic energy distributions; Ion beam degradation; Polymer

1. Introduction

The study of the kinetic energy distributions (KEDs) of molecular fragment ions sputtered from organic surfaces under keV ion bombardment has been developed by several laboratories across the world [1–5]. Indeed, the shape of the KEDs gives important information about the emission processes involved [6]. However, in the case of polymers, few works exist and the forma-

tion of molecular ions from inside the backbone, requiring two bond-scissions at least, is not well understood yet [7]. To improve our knowledge of the relations between the polymer chemistry and the observed secondary ion structures, this work focuses on two simple polymers differing only by their degree of unsaturation: (i) polystyrene – PS, an aromatic hydrocarbon and (ii) polyisobutylene – PIB, a branched aliphatic, saturated hydrocarbon. Ion beam damaged surfaces are also investigated in order to evidence the emission mechanisms related to the pristine/damaged material.

^{*} Corresponding author. Tel.: +32 10 473582; fax: +32 10 473452; e-mail: delcorte@pcpm.ucl.ac.be.

2. Experimental

Monodisperse PS $[-\text{CH}_2-\text{CH}(\text{C}_6\text{H}_5)-]_n$ was received from the University of Liège ($M_n = 60\,000$). PIB $[-\text{CH}_2-\text{C}(\text{CH}_3)_2-]_n$ was purchased from Aldrich Chemie (high molecular weight). Both were prepared as thin films spin-cast on silicon substrates from dilute solutions (~ 1 mg/ml). Prior to deposition, the silicon substrates were rinsed in isopropanol and hexane. The sample cleanliness and purity were tested by XPS (SSI-X-Probe) analysis and no contamination was detected.

The secondary ion mass analyses and the KED measurements were performed in a Time-of-Flight SIMS microprobe-microscope (Charles Evans) using a (5 kHz) pulsed Ga^+ beam (15 kV, 400 pA DC) [8]. For polymer surface degradation studies, continuous bombardment ($5 \times 10^{12} \leq \text{ion fluence } (F) \leq 10^{15}$ ions/cm²) and ToF-SIMS analysis periods (pulsed beam, $F = 10^{12}$ ions/cm²) were alternated [9]. The KED measurements have been described elsewhere [4,10]. Briefly, the secondary ions were first accelerated by a 3 kV potential directly applied on the sample. They were then energy-analysed by a slit placed at the crossover following the first hemispherical electrostatic analyser (passband = 1.5 eV). The different energy windows were selected by varying either the sample voltage or the slit position.

3. Results and discussion

3.1. Effect of the chemical structure of the polymer

The positive secondary ion mass spectra of PIB and PS have been shown respectively in Refs. [9,11]. In the case of PIB, the fingerprint peaks are mostly related to weakly unsaturated $\text{C}_x\text{H}_{2x-1}$ ions ($m/z = 41, 55, 69, 83, 97, 111$). It is important to note that the monomer ion C_4H_8^+ ($m/z = 56$) is intense, even if its particular structure of radical ion makes it rather unstable in theory. The case of PS is quite different: the ions emitted from PS in the range $0 < m/z < 200$ are strongly unsaturated and/or aromatic, C_xH_{x-4} to C_xH_x ions ($m/z = 39, 51, 63, 77, 91, 115, 178, 191$). There-

fore, these two hydrocarbon polymers can be easily distinguished in SIMS.

The KEDs of atomic hydrogen ions sputtered from PIB and PS (Fig. 1(a)) are both rather broad, with a maximum at 3–4 eV, a FWHM close to 8 eV and a high energy tail decreasing slowly with increasing energy. These features are in agreement with collisional sputtering [12]. The discrepancy between the data and the fit by a Sigmund–Thompson law (full line in Fig. 1(a)) may be due to the dependence of the ionisation probability on the particle velocity, which is often reported to scale as $\exp(-v_0/v)$ [13]. Fig. 1(a) shows that the influence of the exact chemical structure of the polymer on the emission of H^+ is not significant.

The energy spectra of the more characteristic ions of PIB and PS, respectively, $\text{C}_7\text{H}_{13}^+$ and C_7H_7^+ are presented in Fig. 1(b). They are narrow, with a steep high energy decrease and a negative apparent energy tail expanding to some tenth of eV. The lat-

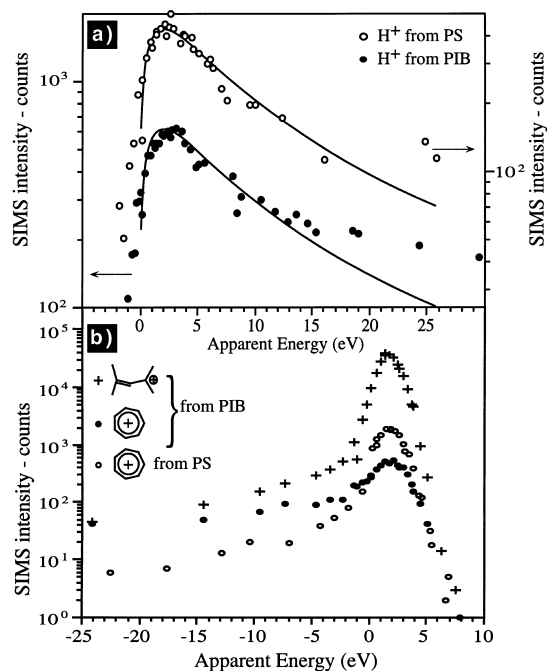


Fig. 1. KEDs of (a) H^+ sputtered from PS and PIB, the continuous line shows the best fit by a Sigmund–Thompson law [$dY/dE \sim E/(E+E_b)^3$, with $E_b = 4.2$ eV]; (b) $\text{C}_7\text{H}_{13}^+$ sputtered from PIB and C_7H_7^+ sputtered from PS and PIB.

ter means that the energy of these ions is lower than the full kinetic energy provided by the 3 kV potential when they reach the first electrostatic analyser. The different FWHMs of the distributions, due to different slopes of the high energy tails, are 2.3 eV for $C_7H_{13}^+$ and 3.5 eV for $C_7H_7^+$ both emitted from PIB and 2.6 eV for $C_7H_7^+$ sputtered from PS. Thus, for a given polymer target (PIB), the emission of fingerprint ions ($C_7H_{13}^+$) is less energetic in average than the emission of highly reorganised ions ($C_7H_7^+$). Consequently, a given ion ($C_7H_7^+$) can be sputtered with rather different mean kinetic energies from different polymer targets, whether it is close to the polymer structure (PS) or not (PIB).

The low energy tail is explained by the fast unimolecular dissociation of metastable parent ions in the acceleration section of the spectrometer [14]. At the dissociation point, such ions split into a neutral and a charged fragment, and the latter continues its way to the detector with a loss of kinetic energy ΔE_k corresponding to the energy left to the neutral particle. The relative contribution of the vacuum formation reaches $\sim 5\%$ of the total integrated intensity for $C_7H_{13}^+$ sputtered from PIB, $\sim 13\%$ for $C_7H_7^+$ sputtered from PS and $\sim 63\%$ for $C_7H_7^+$ sputtered from PIB. This indicates that the relative yield of ions produced in the vacuum is much larger for reorganised ions ($C_7H_7^+$ from PIB). Conversely, the characteristic ions are mostly produced at the surface by a direct emission mechanism.

In the case of hydrocarbon polymers, the similarity between a given molecular ion and the target chemical structure can be estimated by the H/C ratio of the ion. The C_xH_y ions which are close to the PIB (resp. PS) structure will have a H/C ratio (y/x) equal to 2 (resp. 1). With increasing H/C ratio, the FWHM of the KEDs decreases gradually for both polymers (Fig. 2). For a particular H/C ratio, the spreading of the FWHMs is due to the fact that the mean kinetic energy decreases with the ion size, too [5]. In the case of PIB, the FWHM decreases slowly towards a minimum located at $y/x = 2$ or more; for PS, the slope of the decrease is steeper and the minimum is reached at $y/x = 1$. Thus, the average kinetic energy is minimum when the sputtered ion reflects the polymer chemistry and

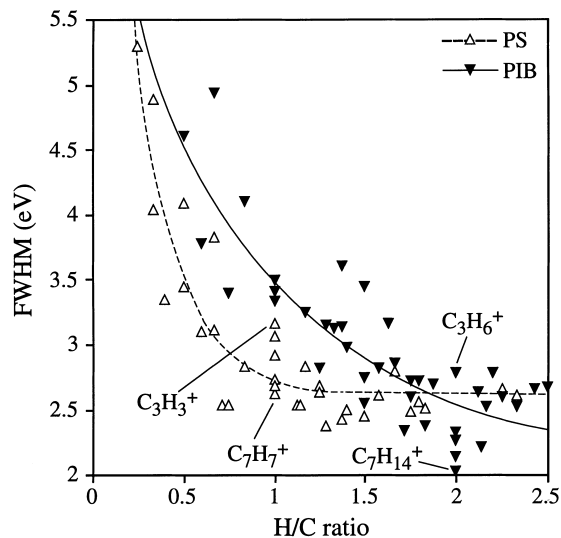


Fig. 2. FWHM of the KEDs of the $C_xH_y^+$ ions sputtered from PS and PIB, as a function of the hydrogen/carbon y/x ratio.

it increases with the degree of fragmentation with respect to this chemical structure.

Although well established in sputtering by keV ions, the collision cascade theory does not predict the steep high energy dependence in Fig. 1(b), nor the gradual evolution in Fig. 2. Nevertheless, this dependence can be interpreted in the frame of collisional sputtering, considering that the removal of the high energy tail is due to the relaxation of the most excited species by further fragmentation [5,15]. Indeed, a violent sputtering event will transfer large amounts of both internal and kinetic energy to the departing polyatomic species. The excess of internal energy (rotation + vibration) may be directly released by fragmentation, while the average kinetic energy will be reduced by a term proportional to $E_k \times \Delta m/m$; where m is the mass of the initial ion and Δm is the mass of the lost fragment. If hydrogen is lost by a large molecular ion, Δm is very small with respect to m and, consequently, the fraction of the kinetic energy lost is insignificant. Due to the depletion of the high energy tail of the KED giving rise to the generation of lighter ions, the remaining precursor-like ions will have low kinetic energies indicating soft emission events. In contrast, ions which have lost hydrogen atoms by fragmentation in the sur-

face region will have relatively higher kinetic energies, because they were produced by more violent emission events. The mean kinetic energy increases with the number of hydrogen atoms lost with respect to the precursor. The same effects were observed with much smaller molecules adsorbed on gold surfaces, indicating similar emission mechanisms [4,5].

3.2. Effect of the beam degradation

The useful secondary ion yields and the FWHMs of the KEDs of the C_xH_y ions sputtered from PIB are presented in Fig. 3, for two different primary ion fluence: (i) $<10^{13}$ ions/cm² (no pre-bombardment) and (ii) 3×10^{14} ions/cm². In both cases, the reorganisation effect is clearly indicated by the periodic variation of the FWHM in each C_xH_i cluster.

With a fluence $<10^{13}$ ions/cm² (static regime), some particular ions exhibit abnormally narrow KEDs: these are mostly radical C_xH_{2x} ions, corresponding exactly to the polymer chemical structure

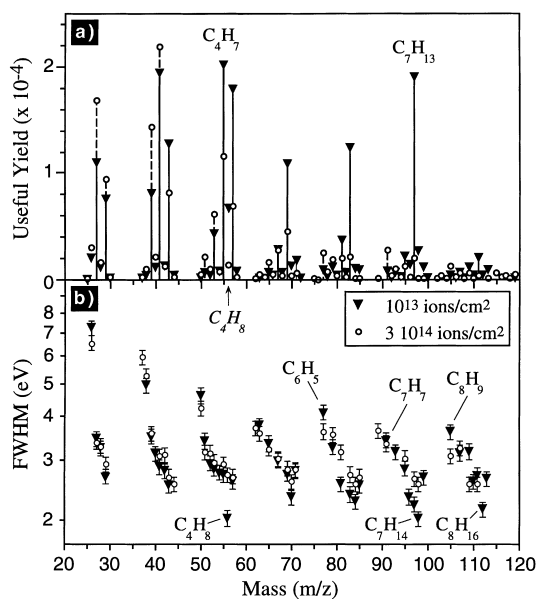


Fig. 3. (a) Useful ion yields [detected secondary ions/primary particle] and (b) FWHMs of the KEDs of the $C_xH_y^+$ ions sputtered from pristine PIB ($F = 10^{13}$ ions/cm²) and pre-bombarded PIB ($F = 3 \times 10^{14}$ ions/cm²).

($m/z = 56, 98, 112$). Fig. 4 shows that the difference between the KED of $C_4H_7^+$ and $C_4H_8^+$ (FWHM = 2.7 and 2.0 eV, resp.) lies mainly in the low energy part of the spectrum, towards negative apparent energies. This means that the production of $C_4H_8^+$ in the vacuum is a minor process in the case of pristine PIB and that the major process is related to a surface-specific emission mechanism. In contrast, a rather important part of the intensity is due to fast unimolecular decay reactions for $C_4H_7^+$ (40% of the integrated peak intensity) and for most of the $C_xH_{y < 2x}$ ions in the mass spectrum. The subtraction of the two curves in Fig. 4 gives an idea about the shape of the metastable ion distribution.

Even if the useful ion yields vary strongly with increasing fluence (Fig. 3(a)), no significant difference can be observed between the FWHMs of the energy spectra measured with 10^{13} ions/cm² and 3×10^{14} ions/cm² (Fig. 3(b)). The only noticeable variation relates to the C_xH_{2x} ions. After pre-bombardment, the FWHM of the $C_4H_8^+$ KED increases and the contribution of the low energy part becomes significant. As the absolute yield of $C_4H_8^+$ is drastically reduced by the degradation (more than four times lower), it can be assumed that the ion bombardment destroys some of the $C_4H_8^+$ initial emission sites and, by the way, that the probability of this ion production by the surface specific mechanism considered above is decreasing with the bombardment fluence [9,16]. The fact that the other formation channel (metastable decay) becomes more important with increasing fluence

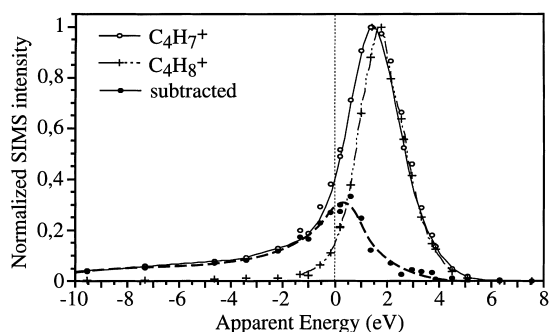


Fig. 4. KEDs of $C_4H_7^+$ and $C_4H_8^+$ sputtered from PIB. The full circles correspond to the subtraction of the two distributions.

(not shown) indicates that the metastable precursors are not so strongly affected by the bombardment. The same arguments apply for $C_7H_{14}^+$ and $C_8H_{16}^+$.

The evolution of the normalised intensities of the C_4H_y ions with the pre-bombardment fluence helps us to understand the secondary ion yields and KEDs measured on the pre-bombarded samples (Fig. 5). In the considered fluence range, two clearly distinct degradation regimes can be observed: (i) below and (ii) above 10^{14} ions/cm². In the first region (Fig. 5(b)), the most characteristic $C_4H_8^+$ peak decreases regularly in relative intensity whereas the others remain stable or even increase ($C_4H_9^+$). This is accompanied by an important increase of the total spectrum intensity, including the C4 series intensity (Fig. 5(a)). The increase of the absolute intensity indicates an augmentation of the ion emission probability in general. This can be explained by the random scission of the polymer chains in the first step of the degradation [17]. In addition, the recombination of the unstable radicals with hydrogen atoms would account for an increase of the relative intensity of the C_xH_{2x+1} ions at the expense of the C_xH_{2x} ions (resp. $C_4H_9^+$ and $C_4H_8^+$ in Fig. 5(b)) in the mass spectra of the pre-bombarded samples. In the second region ($10^{14} < F < 10^{15}$ ions/cm²), the relative intensity of the most saturated ions decreases drastically whereas it increases for the unsaturated ones. This can be interpreted by a gradual dehydrogenation of the bombarded surface [9]. The general intensity loss accompanying dehydrogenation suggests the predominant influence of further branching and/or cross-linking reactions [17] versus dangling bonds stabilisation by hydrogen capture.

The detailed evolution reported in Fig. 5 confirms our interpretation of the $C_xH_{2x}^+$ KED after bombardment with 3×10^{14} ions/cm²: sites of direct emission of $C_xH_{2x}^+$ are destroyed by the bombardment, whereas modified precursors are produced in the first steps of the degradation. This leads to a relative increase of the yield of the $C_xH_{2x+1}^+$ metastable parents after degradation (e.g. $C_4H_9^+$). In this respect, it is interesting to note that hydrogen loss constitutes a favoured metastable decay mechanism for C_xH_y ions sputtered from hydrocarbon polymers [10]. In addition, Fig. 5 as well as the evolution of intensity ratios such as $I(C_xH_y^+)/I(C_xH_{y+2}^+)$ (not shown) indicate that, in contrast with polypropylene [9], dehydrogenation and deep modification of the PIB structure are only initiated beyond 10^{14} ions/cm². This explains why the KED of most of the C_xH_y ions is only slightly affected with a 3×10^{14} ions/cm² pre-bombardment.

4. Conclusion

The broad energy spectrum of H^+ sputtered from hydrocarbon polymers is in agreement with a collisional sputtering process. In addition, it is poorly sensitive to the exact chemical structure of the target. For molecular ions, two important emission channels are evidenced: (i) the direct emission of ions formed at the sample surface; (ii) the unimolecular dissociation of excited parent ions in the vacuum. In general, the broadening of the KED is proportional to the degree of fragmentation of the ion with respect to the polymer structure. The ion formation in the vacuum, indicated by an apparent negative energy tail, is an important process for most of the $C_xH_{y < 2x}$ ions sputtered from PIB. In contrast, for the most characteristic C_xH_{2x} ions, the relative contribution of ion formation in the vacuum is very weak, suggesting the existence of a surface-specific emission process. This

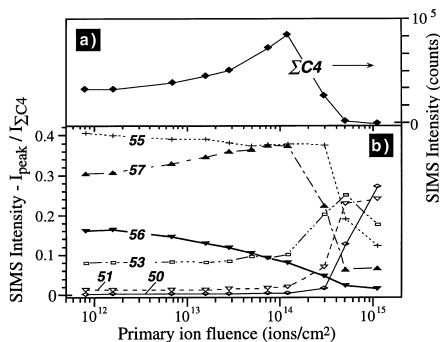


Fig. 5. (a) Evolution of the sum of the $C_4H_y^+$ ions intensities ($\Sigma C4$) as a function of the pre-bombardment fluence (F); (b) Evolution of the normalised intensities of the $C_4H_y^+$ ions as a function of F .

emission process, related to the undamaged polymer material, is strongly reduced on samples pre-bombarded with 3×10^{14} ions/cm². To evidence the effects of a deeper modification of the C_xH_y cluster precursors on the KEDs, future works will require higher pre-bombardment fluences.

Acknowledgements

The authors wish to thank Pr. R. Jérôme at University of Liège for providing the PS beads. S. Errkiba and B.G. Segda are acknowledged for their contribution to the measurements and data processing. This work is supported by the “Action de Recherche Concertée” (94/99-173) of the “Communauté Française de Belgique.” The ToF-SIMS equipment was acquired with the support of the FRFC and the “Région Wallonne” of Belgium.

References

- [1] R. Hoogerbrugge, W.J. van der Zande, P.G. Kistemaker, *Int. J. Mass Spectrom. Ion Processes* 76 (1987) 239.
- [2] R.A. Zubarev, U. Abeywarnna, P. Hakansson, P. Demirev, B.U.R. Sundqvist, *Rapid Commun. Mass Spectrom.* 10 (1996) 1966.
- [3] D.E. Riederer, S.W. Rosencrance, R. Chatterjee, T.D. Dunbar, D.L. Allara, N. Winograd, in: A. Benninghoven, B. Hagenhoff, H.W. Werner (Eds.), *SIMS X Proceedings*, Wiley, New York, 1997, p. 965.
- [4] A. Delcorte, P. Bertrand, *Nucl. Instr. and Meth. B* 115 (1996) 246.
- [5] A. Delcorte, P. Bertrand, *Nucl. Instr. and Meth. B* 117 (1996) 235.
- [6] G. Betz, K. Wien, *Int. J. Mass Spectrom. Ion Processes* 140 (1994) 1.
- [7] G.J. Leggett, J.C. Vickerman, *Int. J. Mass Spectrom. Ion Proc.* 122 (1992) 281.
- [8] B.W. Schueler, *Microsc. Microanal. Microstruct.* 3 (1992) 119.
- [9] A. Delcorte, L.T. Weng, P. Bertrand, *Nucl. Instr. and Meth. B* 100 (1995) 213.
- [10] A. Delcorte, B.G. Segda, P. Bertrand, *Surf. Sci.* 381 (1997) 18.
- [11] X. Vanden Eynde, L.T. Weng, P. Bertrand, *SIMS X Proceedings*, in: (Eds.), A. Benninghoven, B. Hagenhoff, H.W. Werner, Wiley, New York, 1997, p. 727.
- [12] P. Sigmund, in: *Sputtering by Particle Bombardment I*, (Ed.), R. Behrisch, Springer, Berlin, 1981, p. 37.
- [13] M.L. Yu, in: *Sputtering by Particle Bombardment III*, (Eds.), R. Behrisch, K. Wittmaack, Springer, Berlin, 1991, p. 100.
- [14] N.K. Dzhemilev, A.M. Goldenberg, I.V. Veriovkin, S.V. Verkhoturov, *Int. J. Mass. Spetrom Ion Processes* 141 (1995) 209.
- [15] R.A. Haring, R. Pedrys, D.J. Oostra, A. Haring, A.E. De Vries, *Nucl. Instr. and Meth B* 5 (1984) 483.
- [16] I.S. Gilmore, M.P. Seah, *Surf. Interface Anal.* 24 (1996) 746.
- [17] J.-B. Lhoest, J.-L. Dewez, P. Bertrand, *Nucl. Instr. and Meth. B* 105 (1995) 322.